Biochemical and Biophysical Research Communications 427 (2012) 54–59

Contents lists available at SciVerse ScienceDirect

Biochemical and Biophysical Research Communications

journal homepage: www.elsevier.com/locate/ybbrc

Total internal reflection fluorescence imaging of Ca^{2+}-induced Ca^{2+} release in mouse urinary bladder smooth muscle cells

Hisao Yamamura, Yuji Imaizumi *

Department of Molecular & Cellular Pharmacology, Graduate School of Pharmaceutical Sciences, Nagoya City University, Nagoya 467-8603, Japan

ARTICLE INFO

Article history:
Received 14 August 2012
Available online 10 September 2012

Keywords:
TIRF imaging
Ca^{2+}-induced Ca^{2+} release
Smooth muscle
Voltage-dependent Ca^{2+} channel
Ca^{2+} sparklet
Ryanodine receptor

ABSTRACT

In smooth muscles (SMs), cytosolic Ca^{2+} ($[Ca^{2+}]_{cyt}$) dynamics during an action potential are triggered by Ca^{2+} influx through voltage-dependent Ca^{2+} channels (VDCCs) in the plasma membrane. The physiological significance of Ca^{2+} amplification by subsequent Ca^{2+} release through ryanodine receptors (RyRs) from the sarcoplasmic reticulum (SR) is still a matter of topics in SMs. In the present study, depolarization-evoked local Ca^{2+} dynamics in Ca^{2+} microdomain were imaged using total internal reflection fluorescence (TIRF) microscopy in mouse urinary bladder SM cells (UBSMCs). Upon depolarization under whole-cell voltage-clamp, the rapid and local elevation of $[Ca^{2+}]_{cyt}$ was followed by larger $[Ca^{2+}]_{cyt}$ increase with propagation occurred in a limited TIRF zone within ~200 nm from cell surface. The depolarization-evoked $[Ca^{2+}]_{cyt}$ increase in a TIRF zone was abolished or greatly reduced by the pretreatment with Cd^{2+} or ryanodine, respectively. The initial local $[Ca^{2+}]_{cyt}$ increases were mediated by Ca^{2+} influx through single or clustered VDCCs as Ca^{2+} sparklets, and the following step was elicited by Ca^{2+}-induced Ca^{2+} release (CICR) through RyR from SR. The depolarization-induced outward currents, mainly due to large-conductance Ca^{2+}-activated K^+ channel activation, were also markedly reduced by Cd^{2+} and ryanodine. In addition, TIRF analyses showed that the fluorescent signals of individual or clustered VDCC distributed in relatively uniform fashion and that a subset of RyRs in the subplasmalemmal SR also located in TIRF zone. In conclusion, fast TIRF imaging successfully demonstrated two step Ca^{2+} events upon depolarization in Ca^{2+} microdomain of UBSMCs; the initial Ca^{2+} influx as Ca^{2+} sparklets through discrete VDCC or their clusters and the following CICR via the activation of loosely coupled RyRs in SR located in the Ca^{2+} microdomains.

1. Introduction

Cytosolic Ca^{2+} concentration ($[Ca^{2+}]_{cyt}$) is a key factor to regulate a wide range of physiological responses including muscle contraction, secretion, and neurotransmitter release [1]. In smooth muscles (SMs), contractile stimuli elevate $[Ca^{2+}]_{cyt}$ via two major pathways; Ca^{2+} influx through voltage-dependent Ca^{2+} channels (VDCCs) and receptor-operated Ca^{2+} channels in the plasma membrane, and Ca^{2+} release from intracellular Ca^{2+} storage sites through Ca^{2+}-induced Ca^{2+} release (CICR) and inositol 1,4,5-trisphosphate-induced Ca^{2+} release mechanisms [2,3].

Depolarization-evoked local Ca^{2+} transients through ryanodine receptors (RyRs) in the subplasmalemmal sarcoplasmic reticulum (SR), termed as Ca^{2+} hotspots, were successfully imaged using fast-scanning confocal fluorescent microscopy in SM cells (SMCs) freshly isolated from urinary bladder and vas deferens of the guinea-pigs [4,5] and mice [6,7]. Moreover, the Ca^{2+} hotspots activated the large-conductance Ca^{2+}-activated K^+ (BK_{Ca}, also known as $K_{Ca}1.1$) channels in the plasma membrane, contributing to the repolarization phase of an action potential in SMCs. The physiological significance of Ca^{2+} amplification by CICR through mainly RyR type 2 from the SR during depolarization and action potential is still a matter of topics in SMs [8].

Because changes in cytosolic Ca^{2+} signaling are varied spatially and temporally [9], it is necessary for elucidating the physiological significances to obtain Ca^{2+} images with high spatial resolution and fast scanning. In the present study, the depolarization-evoked Ca^{2+} transients during depolarization was imaged with a Ca^{2+}-sensitive fluorescence indicator, fluo-4, using total internal reflection fluorescence (TIRF) microscopy in SMCs freshly isolated from mouse urinary bladder. A TIRF microscope enables detection of the fluorescent-tagged proteins [10,11] including the ion channels [12–16] distributed at the level of the plasmalemma and subplasmalemma in a limited TIRF zone less than 200 nm from the chamber bottom in living cells. Localized Ca^{2+} signaling [17,18] including Ca^{2+} sparklet, which represents the Ca^{2+} transient due

* Corresponding author. Address: Department of Molecular & Cellular Pharmacology, Graduate School of Pharmaceutical Sciences, Nagoya City University, 3-1 Tanabedori Mizuhoku, Nagoya 467-8603, Japan. Fax: +81 52 836 3431.
E-mail address: yimaizum@phar.nagoya-cu.ac.jp (Y. Imaizumi).

0006-291X/$ - see front matter © 2012 Elsevier Inc. All rights reserved.
http://dx.doi.org/10.1016/j.bbrc.2012.08.145

to spontaneous or evoked opening of single or clustered VDCC [19–21], have been also investigated by use of TIRF, whereas the coupling between Ca^{2+} influx through individual VDCC upon depolarization and following local CICR in SMCs has been remained to be confirmed by visualization.

2. Materials and methods

2.1. Ethical approval

All experiments were approved by the Ethics Committee of Nagoya City University and were conducted in accordance with the Guide for the Care and Use of Laboratory Animals of the Japanese Pharmacological Society.

2.2. Cell isolation

Single mouse urinary bladder SMCs (UBSMCs) were prepared using a slight modification of previously described method [6]. In brief, male mice (4–8 weeks old) were quickly killed by cervical dislocation. Urinary bladder was dissected, cleaned of connective tissues, and immersed for 30 min in Ca^{2+}-free Krebs' solution containing 0.2% collagenase (Amano Enzyme, Nagoya, Japan) at 37 °C. After the incubation, the solution was replaced with Ca^{2+}- and collagenase-free Krebs' solution. Myocytes were isolated by gentle agitation with a glass pipette. A few drops of cell suspension were placed in a recording chamber. After these cells were settled, the recording chamber was continuously perfused with the HEPES-buffered solution at a flow rate of 2 ml/min. All experiments were carried out at room temperature (24 ± 1 °C).

2.3. Solutions

The Ca^{2+}-free Krebs' solution had an ionic composition of 112 mM NaCl, 4.7 mM KCl, 1.2 mM $MgCl_2$, 25 mM $NaHCO_3$, 1.2 mM KH_2PO_4, and 14 mM glucose. The pH was adjusted to 7.4 by gassing with a mixture of 95% O_2 and 5% CO_2. The HEPES-buffered solution had an ionic composition of 137 mM NaCl, 5.9 mM KCl, 2.2 mM $CaCl_2$, 1.2 mM $MgCl_2$, 14 mM glucose, and 10 mM HEPES. The pH of the solution was adjusted to 7.4 with 10N NaOH. The pipette solution for electrophysiological recording contained 140 mM KCl, 1 mM $MgCl_2$, 10 mM HEPES, and 2 mM Na_2ATP. The pH was adjusted to 7.2 with 1N KOH. A Ca^{2+} fluorescence indicator was also added to the pipette solution as described below.

2.4. Electrophysiological recording

Electrophysiological experiments were performed using whole-cell patch-clamp configuration with a CEZ-2400 amplifier (Nihon Kohden, Tokyo, Japan), an analog–digital converter (DIGIDATA 1320A; Molecular Devices-Axon Instruments, Foster City, CA), and pCLAMP software (Ver. 8.2; Molecular Devices-Axon Instruments) in single SMCs, as described previously [16]. Depolarizing stimuli from a holding potential of −60 to 0 mV for 50 ms were applied.

2.5. TIRF imaging for $[Ca^{2+}]_{cyt}$ measurement

Two-dimensional Ca^{2+} images were obtained by a TIRF imaging system (Nikon, Tokyo, Japan), which consisted of a fluorescent microscope (ECLIPSE TE2000-U; Nikon), an objective lens (CFI Plan Apo TIRF 60×/1.45, oil immersion; Nikon), an EM-CCD camera (C9100-12; Hamamatsu Photonics, Hamamatsu, Japan), and AQUACOSMOS software (Ver. 2.6; Hamamatsu Photonics), as described previously [16]. Recordings were started at least 3 min after rupturing the patch membrane to make 100 μM fluo-4 (Invitrogen-Molecular Probes, Eugene, USA) for $[Ca^{2+}]_{cyt}$ monitor diffuse into the myocyte from the pipette solution. Fluo-4 was excited with a 488-nm argon laser (Coherent, Santa Clara, USA), and the emission was collected using a filter cube (DM505/BA520; Nikon). Fluorescent signal is described as F/F_0, where F is the averaged fluorescence intensity in the TIRF area during measurement and F_0 is that before the start of depolarizing stimulus. TIRF images with the resolution of 178 nm per pixel (x–y) and less than 200 nm (z) were scanned every 4.2 ms.

2.6. TIRF imaging for single-molecule analysis

Single SMCs were fluorescently stained with 100 nM DM-BODIPY (−)-dihydropyridine (Invitrogen-Molecular Probes) for VDCC or 100 nM BODIPY FL-X ryanodine (Invitrogen-Molecular Probes) for RyR for approximately 10 min at room temperature, and then the excessive indicator was thoroughly washed away from intra/extracellular spaces for over 10 min. These fluorescent signals were obtained by a method similar to fluo-4 imaging.

2.7. Immunocytochemistry

Single SMCs were fixed with 4% paraformaldehyde in phosphate-buffered saline (PBS) for 10 min at room temperature, and excessive paraformaldehyde was removed thoroughly with PBS. These cells were treated with PBS containing 0.2% Triton X-100, 1% normal goat serum (NGS, DakoCytomation, Glostrup, Denmark), and primary antibody for VDCCα1C subunit (1:100 dilution; ACC-003, Alomone Lab, Jerusalem, Israel) for 12 h at 4 °C. After washing repeatedly in PBS, these were covered with PBS containing 0.2% Triton X-100, 1% NGS, and Alexa Fluor 488-labeled secondary antibody solution (1:1000 dilution; Invitrogen-Molecular Probes) for 1 h at room temperature and then rinsed with PBS. TIRF images were obtained as mentioned above.

2.8. Chemicals

Pharmacological reagents were obtained from Sigma–Aldrich (St. Louis, USA) except for cadmium chloride, ryanodine (Wako Pure Chemical, Osaka, Japan), HEPES (Dojin, Kumamoto, Japan), and iberiotoxin (Peptide Institute, Osaka, Japan).

2.9. Statistics

Pooled data are shown as the mean ± S.E. Statistical significance between two groups was determined by Student's t-test. Significant difference is expressed as $^{*}p < 0.05$ or $^{**}p < 0.01$ in the figures.

3. Results and discussion

3.1. TIRF imaging of local Ca^{2+} transients during depolarization

The depolarization-evoked local Ca^{2+} transients, Ca^{2+} hotspots, via CICR through RyRs in the subplasmalemmal SR were imaged using TIRF microscopy in mouse UBSMCs. When myocytes were depolarized for 50 ms from a holding potential of −60 to 0 mV, several localized Ca^{2+} elevation as fluo-4 signals occurred in the internal surface of plasma membrane at 4.2 and 8.4 ms after the start of depolarization (Fig. 1A and B). At 12.6 ms after the depolarization, $[Ca^{2+}]_{cyt}$ was amplified in the TIRF area. The rate of $[Ca^{2+}]_{cyt}$ change reached the peak within 16 ms. The elevation of $[Ca^{2+}]_{cyt}$ returned to the resting level with a half decay time of approximately 500 ms. In confocal imaging that had the resolution of 0.33 × 0.27 μm per pixel and 1.2–1.5 μm to Z-axis direction and

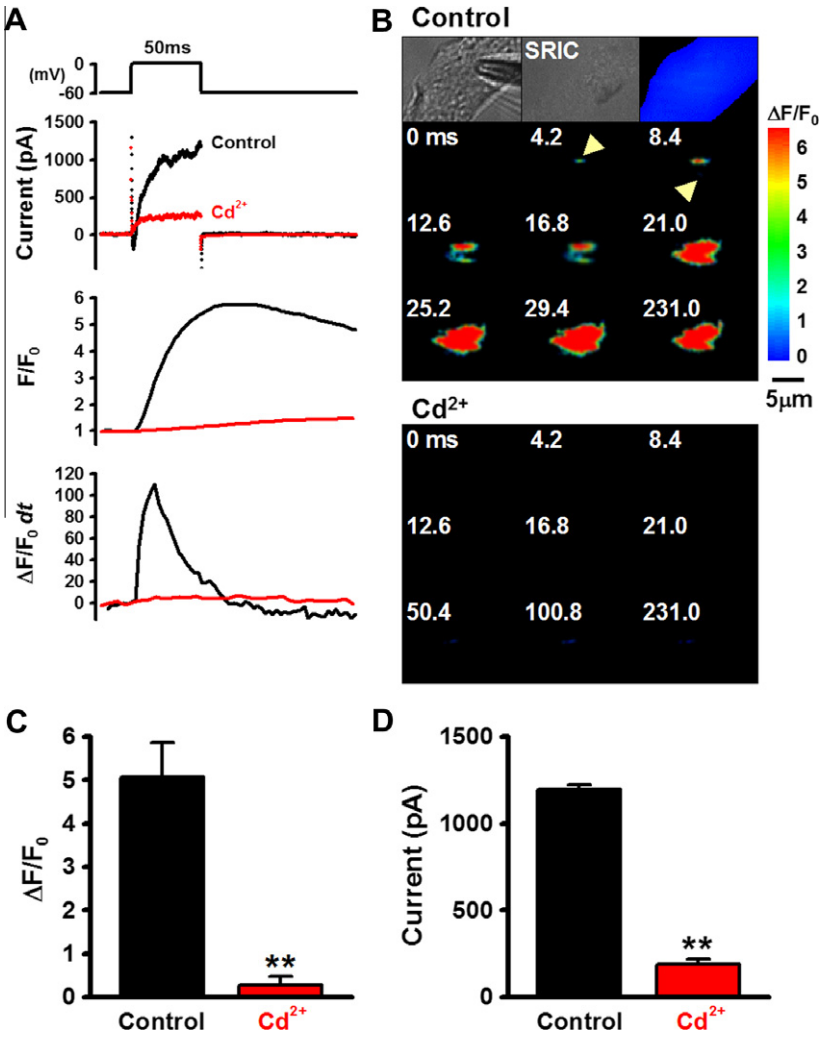

Fig. 1. TIRF imaging of local Ca^{2+} transients during depolarization. Single smooth muscle cells of mouse urinary blabber (UBSMCs) were enzymatically isolated and then loaded with a Ca^{2+}-sensitive fluorescent indicator, 100 μM fluo-4, from a recording pipette. Myocytes were depolarized from a holding potential of −60 to 0 mV for 50 ms using whole-cell patch-clamp techniques. Ca^{2+} images in a limited TIRF zone less than 200 nm from the chamber bottom were acquired every 4.2 ms. (A) Membrane current (*upper*), $[Ca^{2+}]_{cyt}$ (F/F_0) in a TIRF zone (*middle*), and the rate of $[Ca^{2+}]_{cyt}$ change ($\Delta F/F_0 dt$) (*bottom*) during membrane depolarization in the absence (*black*) and presence (*red*) of 100 μM Cd^{2+} are plotted against time. F was calculated by the averaged fluorescence intensity of fluo-4 from the TIRF zone and normalized by the F_0 obtained before the depolarization (F/F_0). The application of Cd^{2+} abolished the increases in $[Ca^{2+}]_{cyt}$ and outward current by depolarization. (B) TIRF images during depolarization in the absence (*Control*) and presence of Cd^{2+} are shown with time. The depolarizing pulse started at 0 ms. Upon membrane depolarization, $[Ca^{2+}]_{cyt}$ immediately increased at several local areas (Ca^{2+} sparklets as Ca^{2+} influx through single or clustered VDCCs; indicated by *arrowheads*) followed by larger increase in $[Ca^{2+}]_{cyt}$ (CICR as Ca^{2+} hotspots). The depolarization-elicited increase in $[Ca^{2+}]_{cyt}$ was disappeared by the application of Cd^{2+}. The transmitted image, surface reflective interference contrast (SRIC) image, and the myocyte shape are also arranged (*first line in Control*). (C & D) Effects of Cd^{2+} on $[Ca^{2+}]_{cyt}$ increase (C) and the peak amplitude of outward currents (D) evoked by depolarization are summarized. Experimental data were obtained from five myocytes. The statistical significance is expressed as $^{**}p < 0.01$ vs. control.

scanned every 8.25 ms as reported previously [4–6], local Ca^{2+} transients at 8–10 ms after depolarization stimulation were identified as CICR in SMCs. With lower spatial resolution of confocal imaging, it was difficult to separate the component of Ca^{2+} influx through VDCCs from local Ca^{2+} transients evoked by depolarization. In this study, TIRF imaging with higher spatiotemporal resolution clearly demonstrated the depolarization-evoked Ca^{2+} influx through VDCCs prior to CICR in SMCs. In the measurement of Ca^{2+} sparklet, which represents spontaneous or evoked opening of single or clustered VDCC, the pipette solution contains EGTA at a high concentration (>5 mM) to prevent CICR in cerebral arterial SMCs [21,22]. In the present study, the pipette solution did not contained EGTA and, thereby, clearly showed both initial Ca^{2+} elevation, which corresponds to evoked Ca^{2+} sparklet [21,23], and following Ca^{2+} hotspot, together with BK_{Ca} channel currents during depolarization. The delay of CICR occurrence from the sparklet was about 4–5 ms, which presumably corresponding to the loose coupling between them in contrast to that in cardiac myocytes [24].

3.2. Blockage by Cd^{2+} on depolarization-induced Ca^{2+} influx

It is expected that the rapid elevation of $[Ca^{2+}]_{cyt}$ during depolarization is caused by Ca^{2+} influx via VDCCs. Effects of Cd^{2+}, a blocker of VDCCs, on changes in $[Ca^{2+}]_{cyt}$ and membrane current by depolarization were, therefore, examined in mouse UBSMCs. When the myocytes were again depolarized 5 min after the first depolarization (as control), changes in $[Ca^{2+}]_{cyt}$ in the presence of 100 μM Cd^{2+} were monitored (Fig. 1A and B). The application of Cd^{2+} almost abolished the elevation of $[Ca^{2+}]_{cyt}$ by depolarization (0.28 ± 0.20 $\Delta F/F_0$, $n = 5$, $p < 0.01$ vs. control of 5.06 ± 0.81 $\Delta F/F_0$; Fig. 1C). Additionally, the application of Cd^{2+} significantly reduced

the amplitude of outward currents from 1198 ± 25 to 189 ± 28 pA ($n = 5$, $p < 0.01$; Fig. 1D).

3.3. Inhibitory effects of ryanodine on CICR during depolarization

Effects of ryanodine, an inhibitor of RyRs, on changes in $[Ca^{2+}]_{cyt}$ and membrane current by depolarization were examined in mouse urinary bladder myocytes. When myocytes were depolarized for 50 ms from a holding potential of −60 to 0 mV, localized Ca^{2+} transients were detected in the surface of plasma membrane at 4.2 ms after the start of depolarization (Fig. 2A and B). Subsequently, larger $[Ca^{2+}]_{cyt}$ increase was induced in the TIRF area at 12.6 ms after the depolarization pulse. The elevation of $[Ca^{2+}]_{cyt}$ recovered to the resting level within 3 s after the repolarization. When these cells were again depolarized after the pretreatment with 10 μM ryanodine for 10 min, changes in $[Ca^{2+}]_{cyt}$ and membrane currents were observed (Fig. 2A and B). In the presence of ryanodine, rapid Ca^{2+} transient was observed at 4.2 ms whereas larger increase in $[Ca^{2+}]_{cyt}$ was not detected, indicating that only Ca^{2+} influx through VDCCs was observed but subsequent CICR was blocked by ryanodine. The pretreatment with ryanodine markedly reduced the elevation of $[Ca^{2+}]_i$ by depolarization (0.88 ± 0.39 $\Delta F/F_0$, $n = 6$, $p < 0.05$ vs. control of 4.10 ± 0.69 $\Delta F/F_0$; Fig. 2C). Similarly, the application of Cd^{2+} significantly decreased the amplitude of outward currents from 1148 ± 50 to 373 ± 94 pA ($n = 6$, $p < 0.01$; Fig. 2D). The Ca^{2+} transients in the presence of ryanodine apparently correspond to those of evoked Ca^{2+} sparklets, which were also recorded as TIRF images under the conditions where CICR does not occur in vascular SMCs [21,23].

3.4. Activation of BK_{Ca} channels by local Ca^{2+} transients

BK_{Ca} channels are expressed mainly in excitable cells such as neurons and SMs and activated by both membrane depolarization and elevated $[Ca^{2+}]_{cyt}$ [25]. Because membrane hyperpolarization mediated by BK_{Ca} channel activation protects cells from excessive

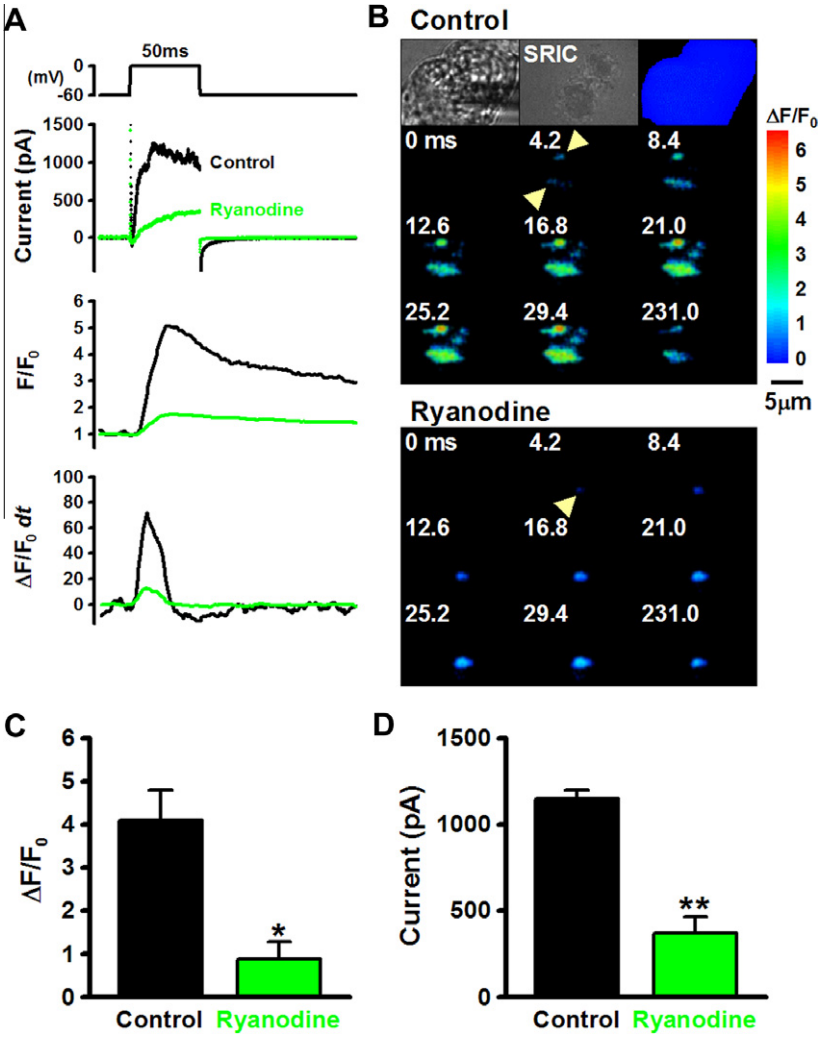

Fig. 2. TIRF imaging of Ca^{2+} influx and release during depolarization. Effects of ryanodine, an inhibitor of RyRs, on the depolarization-evoked local Ca^{2+} transients were examined in mouse UBSMCs. Myocytes were depolarized from a holding potential of −60 to 0 mV for 50 ms. TIRF images of myocytes stained with fluo-4 were acquired every 4.2 ms. (A) Membrane current (*upper*), $[Ca^{2+}]_{cyt}$ (F/F_0) in a TIRF zone (*middle*), and the rate of $[Ca^{2+}]_{cyt}$ change ($\Delta F/F_0 dt$) (*bottom*) by membrane depolarization before (*black*) and after (*green*) the application of 10 μM ryanodine are plotted against time. The pretreatment with ryanodine reduced the elevation of $[Ca^{2+}]_{cyt}$ and the amplitude of outward current during depolarization. (B) TIRF images during depolarization in the absence (*Control*) and presence of ryanodine are shown with time. TIRF images obtained at 4.2 ms after the start of depolarization show local Ca^{2+} transients (evoked Ca^{2+} sparklets) regardless the presence of ryanodine (*arrowhead*). The transmitted image, surface reflective interference contrast (SRIC), and shape of the myocyte are also arranged (*first line in Control*). Note larger increase in $[Ca^{2+}]_{cyt}$ (Ca^{2+} release) elicited by depolarization was disappeared by the external application of ryanodine, whereas rapid $[Ca^{2+}]_{cyt}$ rise (evoked Ca^{2+} sparklets) was still remained. (C & D) Effects of ryanodine on $[Ca^{2+}]_{cyt}$ increase (C) and outward current amplitude (D) evoked by depolarization are summarized. Experimental data were obtained from six myocytes. The statistical significance is expressed as $^*p < 0.05$ or $^{**}p < 0.01$ vs. control.

excitability and Ca^{2+} overload by closing VDCCs, this channel is thought to contribute to the regulation of $[Ca^{2+}]_{cyt}$ as a key molecule in the negative-feedback mechanism [26]. In this study, membrane currents were simultaneously recorded with Ca^{2+} images by whole-cell voltage-clamp configuration in SMCs of mouse urinary bladder. The outward currents were mainly due to the activation of BK_{Ca} channels sensitive to 100 nM iberiotoxin and closely paralleled the $[Ca^{2+}]_{cyt}$ rise, as reported previously [4,5]. The depolarization-evoked outward currents were markedly reduced by Cd^{2+} and ryanodine. These results also confirmed the previous finding that the major Ca^{2+} source for BK_{Ca} activation induced by depolarization or an action potential is Ca^{2+} release from SR via CICR in UBSMCs. In SMs, two types of local Ca^{2+} events, Ca^{2+} hotspots attributable to depolarization-evoked CICR [4,5] and Ca^{2+} sparks due to spontaneous Ca^{2+} release [27], play crucial roles in the regulation of contraction and relaxation, respectively [28,29]. These two Ca^{2+} events occur in the same distinct local areas in SMs to couple with BK_{Ca} channel activity and contribute to the repolarization phase of action potential and spontaneous transient outward currents, respectively [5].

3.5. Spatial distribution of VDCC and RyR

To analyze spatial distribution of VDCC in the surface of plasma membrane and RyR in the subplasmalemmal SR, TIRF imaging was performed using these fluorescent markers in mouse UBSMCs. When myocytes were incubated with 100 nM DM-BODIPY (−)-dihydropyridine, a fluorescent marker of L-type VDCC, the fluorescent signals of individual channel unit or their clusters distributed in relatively uniform fashion in the TIRF images ($n = 10$; Fig. 3A). Similar uniform distribution was observed in TIRF images using specific VDCCα1C antibody (1:100, $n = 3$). On the other hand, signals of RyRs stained with 100 nM BODIPY FL-X ryanodine were also detected in the limited TIRF region ($n = 11$; Fig. 3B), which were limited within 200 nm from the cell surface.

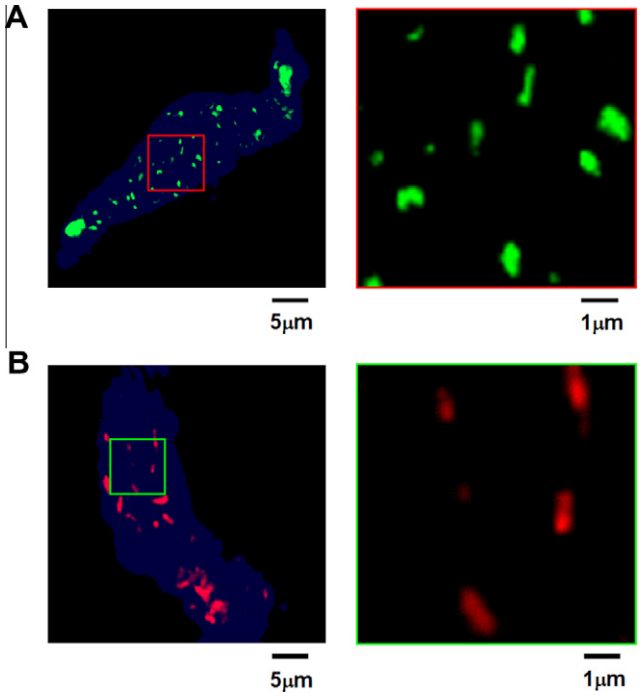

Fig. 3. Spatial distribution of VDCC and RyR. Spatial distributions of VDCC and RyR were imaged by TIRF microscopy in single UBSMCs. (A) The expression of VDCC in plasma membrane was visualized with 100 nM DM-BODIPY (−)-dihydropyridine. Note that the fluorescent signals of individual VDCC unit or their clusters were relatively uniformly-distributed in a TIRF image. (B) The distribution of RyR in the subplasmalemmal region was stained with 100 nM BODIPY FL-X ryanodine. The fluorescent signals of their fragments (or individual unit) were able to detect in a TIRF zone, which was within 200 nm from the cell surface.

In SMs, BK_{Ca} channels in the plasma membrane and RyR type 2 in the junctional SR have been considered as intrinsic components of the Ca^{2+} microdomain in plasmalemmal and subplasmalemmal regions, where signaling mediated by changes in membrane potential and local $[Ca^{2+}]_{cyt}$ is communicated with high efficiency. Caveolae, Ω-shaped invaginations on the membrane surface (50–100 nm in diameter), may be essential for the compartmentalization of signaling molecules during physiological events [3,30]. It has been suggested that caveolae are junctional functions in plasmalemma to specific SR and work as Ca^{2+} hotspot and spark sites [7,31]. Also the aggregation of BK_{Ca} channels in caveolae, which abundantly contain caveolin proteins, has been suggested in SMCs [16,32]. In contrast, the distribution and size of fluorescent particles of VDCC in the surface of plasma membrane was relatively uniform as shown in Fig. 3A. The relationships between VDCC activity, local SR Ca^{2+} content and Ca^{2+} release amount through RyR from in a microdomain SR are still hot issue in SMCs [2,23].

In conclusion, Ca^{2+} influx through VDCCs upon depolarization has been suggested to be a trigger of CICR and result in excitation–contraction coupling under physiological conditions in UBSMCs, which are highly excitable. Using TIRF imaging techniques, the evoked Ca^{2+} sparklet through single or clustered L-type VDCC and following CICR via activation of RyRs in the subplasmalemmal SR in a Ca^{2+} microdomain were visualized and analyzed as loosely coupled two steps for Ca^{2+} signal amplification in UBSMCs.

Acknowledgments

This investigation was supported by a Grant-in-Aid for Scientific Research on Priority Areas (20056027; to Y.I.) from the Ministry of Education, Culture, Sports, Science, and Technology, and Grant-in-Aids for Scientific Research (B) (23390020; to Y.I.) and Young Scientists (B) (23790092; to H.Y.) from the Japan Society for the Promotion of Science. This work was also supported by a Grant-in-Aid from Takeda Science Foundation (to H.Y.).

References

[1] R.W. Tsien, R.Y. Tsien, Calcium channels, stores, and oscillations, Annu. Rev. Cell Biol. 6 (1990) 715–760.
[2] S. Wray, T. Burdyga, Sarcoplasmic reticulum function in smooth muscle, Physiol. Rev. 90 (2010) 113–178.
[3] D. Narayanan, A. Adebiyi, J.H. Jaggar, Inositol trisphosphate receptors in smooth muscle cells, Am. J. Physiol. Heart Circ. Physiol. 302 (2012) H2190–H2210.
[4] Y. Imaizumi, Y. Torii, Y. Ohi, N. Nagano, K. Atsuki, H. Yamamura, K. Muraki, M. Watanabe, T.B. Bolton, Ca^{2+} images and K^+ current during depolarization in smooth muscle cells of the guinea-pig vas deferens and urinary bladder, J. Physiol. 510 (1998) 705–719.
[5] Y. Ohi, H. Yamamura, N. Nagano, S. Ohya, K. Muraki, M. Watanabe, Y. Imaizumi, Local Ca^{2+} transients and distribution of BK channels and ryanodine receptors in smooth muscle cells of guinea-pig vas deferens and urinary bladder, J. Physiol. 534 (2001) 313–326.
[6] K. Morimura, Y. Ohi, H. Yamamura, S. Ohya, K. Muraki, Y. Imaizumi, Two-step Ca^{2+} intracellular release underlies excitation–contraction coupling in mouse urinary bladder myocytes, Am. J. Physiol. Cell Physiol. 290 (2006) C388–C403.
[7] S. Hotta, H. Yamamura, S. Ohya, Y. Imaizumi, Methyl-β-cyclodextrin prevents Ca^{2+}-induced Ca^{2+} release in smooth muscle cells of mouse urinary bladder, J. Pharmacol. Sci. 103 (2007) 121–126.
[8] S. Hotta, K. Morimura, S. Ohya, K. Muraki, H. Takeshima, Y. Imaizumi, Ryanodine receptor type 2 deficiency changes excitation–contraction coupling and membrane potential in urinary bladder smooth muscle, J. Physiol. 582 (2007) 489–506.
[9] H. Cheng, W.J. Lederer, Calcium sparks, Physiol. Rev. 88 (2008) 1491–1545.
[10] M. Ueda, Y. Sako, T. Tanaka, P. Devreotes, T. Yanagida, Single-molecule analysis of chemotactic signaling in *Dictyostelium* cells, Science 294 (2001) 864–867.
[11] C. Nakada, K. Ritchie, Y. Oba, M. Nakamura, Y. Hotta, R. Iino, R.S. Kasai, K. Yamaguchi, T. Fujiwara, A. Kusumi, Accumulation of anchored proteins forms membrane diffusion barriers during neuronal polarization, Nat. Cell Biol. 5 (2003) 626–632.

[12] E. Oancea, J.T. Wolfe, D.E. Clapham, Functional TRPM7 channels accumulate at the plasma membrane in response to fluid flow, Circ. Res. 98 (2006) 245–253.
[13] R.M. Luik, M.M. Wu, J. Buchanan, R.S. Lewis, The elementary unit of store-operated Ca^{2+} entry: local activation of CRAC channels by STIM1 at ER-plasma membrane junctions, J. Cell. Biol. 174 (2006) 815–825.
[14] T.T. Lambers, E. Oancea, T. de Groot, C.N. Topala, J.G. Hoenderop, R.J. Bindels, Extracellular pH dynamically controls cell surface delivery of functional TRPV5 channels, Mol. Cell Biol. 27 (2007) 1486–1494.
[15] V. Nechyporuk-Zloy, P. Dieterich, H. Oberleithner, C. Stock, A. Schwab, Dynamics of single potassium channel proteins in the plasma membrane of migrating cells, Am. J. Physiol. Cell Physiol. 294 (2008) C1096–C1102.
[16] H. Yamamura, C. Ikeda, Y. Suzuki, S. Ohya, Y. Imaizumi, Molecular assembly and dynamics of fluorescent protein-tagged single $K_{Ca}1.1$ channel in expression system and vascular smooth muscle cells, Am. J. Physiol. Cell Physiol. 302 (2012) C1257–C1268.
[17] A. Demuro, I. Parker, "Optical patch-clamping": single-channel recording by imaging Ca^{2+} flux through individual muscle acetylcholine receptor channels, J. Gen. Physiol. 126 (2005) 179–192.
[18] D. Yamazaki, Y. Tabara, S. Kita, H. Hanada, S. Komazaki, D. Naitou, A. Mishima, M. Nishi, H. Yamamura, S. Yamamoto, S. Kakizawa, H. Miyachi, T. Miyata, Y. Kawano, K. Kamide, T. Ogihara, A. Hata, S. Umemura, M. Soma, N. Takahashi, Y. Imaizumi, T. Miki, T. Iwamoto, H. Takeshima, TRIC-A channels in vascular smooth muscle contribute to blood pressure maintenance, Cell Metab. 14 (2011) 231–241.
[19] M.F. Navedo, G.C. Amberg, V.S. Votaw, L.F. Santana, Constitutively active L-type Ca^{2+} channels, Proc. Natl. Acad. Sci. USA 102 (2005) 11112–11117.
[20] L.F. Santana, M.F. Navedo, G.C. Amberg, M. Nieves-Cintron, V.S. Votaw, C.A. Ufret-Vincenty, Calcium sparklets in arterial smooth muscle, Clin. Exp. Pharmacol. Physiol. 35 (2008) 1121–1126.
[21] M.F. Navedo, Y. Takeda, M. Nieves-Cintron, J.D. Molkentin, L.F. Santana, Elevated Ca^{2+} sparklet activity during acute hyperglycemia and diabetes in cerebral arterial smooth muscle cells, Am. J. Physiol. Cell Physiol. 298 (2010) C211–C220.
[22] G.C. Amberg, M.F. Navedo, M. Nieves-Cintron, J.D. Molkentin, L.F. Santana, Calcium sparklets regulate local and global calcium in murine arterial smooth muscle, J. Physiol. 579 (2007) 187–201.
[23] Y. Takeda, M.A. Nystoriak, M. Nieves-Cintron, L.F. Santana, M.F. Navedo, Relationship between Ca^{2+} sparklets and sarcoplasmic reticulum Ca^{2+} load and release in rat cerebral arterial smooth muscle, Am. J. Physiol. Heart Circ. Physiol. 301 (2011) H2285–H2294.
[24] M.I. Kotlikoff, Calcium-induced calcium release in smooth muscle: the case for loose coupling, Prog. Biophys. Mol. Biol. 83 (2003) 171–191.
[25] L. Salkoff, A. Butler, G. Ferreira, C. Santi, A. Wei, High-conductance potassium channels of the SLO family, Nat. Rev. Neurosci. 7 (2006) 921–931.
[26] M.T. Nelson, J.M. Quayle, Physiological roles and properties of potassium channels in arterial smooth muscle, Am. J. Physiol. 268 (1995) C799–C822.
[27] M.T. Nelson, H. Cheng, M. Rubart, L.F. Santana, A.D. Bonev, H.J. Knot, W.J. Lederer, Relaxation of arterial smooth muscle by calcium sparks, Science 270 (1995) 633–637.
[28] Y. Imaizumi, Y. Ohi, H. Yamamura, S. Ohya, K. Muraki, M. Watanabe, Ca^{2+} spark as a regulator of ion channel activity, Jpn. J. Pharmacol. 80 (1999) 1–8.
[29] J.H. Jaggar, V.A. Porter, W.J. Lederer, M.T. Nelson, Calcium sparks in smooth muscle, Am. J. Physiol. Cell Physiol. 278 (2000) C235–C256.
[30] L.M. Popescu, M. Gherghiceanu, E. Mandache, D. Cretoiu, Caveolae in smooth muscles: nanocontacts, J. Cell Mol. Med. 10 (2006) 960–990.
[31] X. Cheng, J.H. Jaggar, Genetic ablation of caveolin-1 modifies Ca^{2+} spark coupling in murine arterial smooth muscle cells, Am. J. Physiol. Heart Circ. Physiol. 290 (2006) H2309–H2319.
[32] A.M. Brainard, A.J. Miller, J.R. Martens, S.K. England, Maxi-K channels localize to caveolae in human myometrium: a role for an actin-channel-caveolin complex in the regulation of myometrial smooth muscle K^+ current, Am. J. Physiol. Cell Physiol. 289 (2005) C49–C57.